HHS Public Access

Author manuscript

J Orthop Res. Author manuscript; available in PMC 2019 February 01.

Published in final edited form as:

J Orthop Res. 2018 February ; 36(2): 653–662. doi:10.1002/jor.23665.

Mechanical loading disrupts osteocyte plasma membranes which initiates mechanosensation events in bone

Kanglun Yu[1], **David P. Sellman**[1], **Anoosh Bahraini**[1], **Mackenzie L. Hagan**[1], **Ahmed Elsherbini**[1], **Kayce T. Vanpelt**[1], **Peyton L. Marshall**[1], **Mark W. Hamrick**[1], **Anna McNeil**[1], **Paul L. McNeil**[1], and **Meghan E. McGee-Lawrence**[1,2,+]

[1]Department of Cellular Biology and Anatomy, Medical College of Georgia, Augusta University, 1120 15th St, Augusta, GA

[2]Department of Orthopaedic Surgery, Medical College of Georgia, Augusta University, 1120 15th St, Augusta, GA

Abstract

Osteocytes sense loading in bone, but their mechanosensation mechanisms remain poorly understood. Plasma membrane disruptions (PMD) develop with loading under physiological conditions in many cell types (e.g., myocytes, endothelial cells). These PMD foster molecular flux across cell membranes that promotes tissue adaptation, but this mechanosensation mechanism had not been explored in osteocytes. Our goal was to investigate whether PMD occur and initiate consequent mechanotransduction in osteocytes during physiological loading. We found that osteocytes experience PMD during *in vitro* (fluid flow) and *in vivo* (treadmill exercise) mechanical loading, in proportion to the level of stress experienced. In fluid flow studies, osteocyte PMD preferentially formed with rapid as compared to gradual application of loading. In treadmill studies, osteocyte PMD increased with loading in weight bearing locations (tibia), but this trend was not seen in non-weight bearing locations (skull). PMD initiated osteocyte mechanotransduction including calcium signaling and expression of c-fos, and repair rates of these PMD could be enhanced or inhibited pharmacologically to alter downstream mechanotransduction and osteocyte survival. PMD may represent a novel mechanosensation pathway in bone and a target for modifying skeletal adaptation signaling in osteocytes.

Keywords

bone; skeleton; osteocyte; mechanotransduction; cell wounding; mechanical loading

[+]Corresponding Author: Meghan E. McGee-Lawrence, Ph.D., Department of Cellular Biology and Anatomy, Medical College of Georgia, Augusta University, 1120 15th St, Augusta GA 30912, Phone: (706) 446-0128, Fax: (706) 721-6120, mmcgeelawrence@augusta.edu.

Disclosure: All authors have no conflicts of interest.

Author Contributions: Experimental design: MWH, PLM, and MEML. Data collection and analysis: KY, DPS, AB, MLH, AE, KTV, PLM, AM, PLM, MEML. Drafting manuscript: PLM and MEML. All authors have read and approved the final submitted manuscript.

Introduction

Bone adapts to imposed loads. It is important to understand how bone senses changes in its mechanical environment and initiates an appropriate adaptive response, as defects in bone mechanosensing can contribute to the development of osteoporosis and skeletal fractures with aging and immobility(1). Osteocytes, the primary mechanosensor in bone, are thought to sense loading primarily via fluid flow in the lacunocanalicular system, but the mechanisms behind this phenomenon are not fully understood. Several potential osteocyte mechanosensation mechanisms observed *in vitro* have not fully explained *in vivo* skeletal adaptation (2–5). An intracellular Ca^{2+} spike is one of the earliest responses triggered in a mechanically loaded osteocyte, and this response requires extracellular Ca^{2+} (6), but the mechanism for extracellular Ca^{2+} entry has not been fully explained (7).

In many cell types, such as myocytes, physiological mechanical loading (e.g., treadmill exercise for the musculoskeletal system) (8, 9) creates tears in the cell membrane called plasma membrane disruptions (PMD) (8). These survivable, nanometer- to micron-sized tears promote molecular flux across the cell membrane, allowing Ca^{2+} entry and release of growth factors like FGFs (10). The initial inrush of extracellular Ca^{2+} through a PMD triggers activation of calpains, depolarization of voltage-gated calcium channels, and mobilization of repair machinery including Annexin proteins (11) which seal the PMD in a timeframe of 1 to 2 minutes. PMD and associated repair initiate signaling both in the wounded cell and in non-wounded adjacent neighbors (12), instigating mechanotransduction including up-regulation of early response genes like c-fos and Cox-2 (8, 13), and release of nitric oxide (14) and prostaglandins. This same mechanotransduction cascade occurs in mechanically loaded osteocytes (15), but the possibility that PMD initiate mechanosensing in osteocytes has not been explored. The objectives of this study were to 1) investigate the fundamental question of whether membrane disruptions occur in osteocytes with physiological loading, 2) determine whether mechanotransduction signaling is activated in PMD-affected osteocytes, and 3) quantify the osteocyte PMD repair response and its potential effects on mechanotransduction.

Materials & Methods

Cell culture

MLO-Y4 cells, courtesy of Dr. Lynda Bonewald were maintained in growth medium (α-MEM (Invitrogen)+5% fetal bovine serum (FBS, Atlanta Biologicals)+5% bovine calf serum (HyClone)+1% Penicillin/Streptomycin). Primary osteocytes were isolated from serial digestion of 8 week old wildtype C57BL/6 mouse long bones as we previously reported (16) and were maintained in growth medium as described above. OCY454 cells, courtesy of Dr. Paola Divieti-Pajevic, were maintained in growth medium (α-MEM+10% FBS+1% Antibiotic/antimycotic (Gibco)) and handled according to published protocols (17). Briefly, OCY454 cells were maintained at 33°C on collagen coated plates, and differentiated at 37°C on non-coated plates for 2 weeks prior to the onset of experiments to promote an osteocytic phenotype, according to the recommended protocol for these cells.

Fluid flow shear stress: Flexcell Streamer

MLO-Y4 cells were seeded 72 hours prior to experiments onto type 1 collagen-coated slides (18); cells were 70% confluent at the time of experiments. For studies utilizing reduced serum (1% FBS, 1% BCS, 1 mg/mL bovine serum albumin), cells were switched to lower-serum medium 24 hours prior to experiments. Media with fluorescein-conjugated dextran (10 kDa, 1 mg/mL) was applied to control cells (slides in static dishes) or used to apply fluid shear stresses (10 to 30 dynes/cm^2) via laminar flow in a parallel plate flow chamber (Streamer, Flexcell) for as few as 7 minutes or as long as 2 hours. After each experiment, slides were rinsed in phosphate buffered saline (PBS); cells that repair PMD will retain the dye after washing (19). Slides were imaged on a multi-photon confocal microscope (Zeiss); please see Supplementary Methods for additional details. The percentage of PMD-affected cells was quantified with image analysis software (Bioquant Osteo).

Fluid flow shear stress: Glycotech flow chamber

MLO-Y4 cells were seeded 4 days prior to experiments onto type 1 collagen coated dishes; cells were 70% confluent at the time of experiments. PMD tracers including fluorescein-conjugated dextran (10 kDa, 1 mg/mL) or lipophilic FM dye (FM1-43 or FM4-64, 2 μM) were added to media immediately prior to experiments. Cells were exposed to fluid flow shear stress (30 or 40 dynes/cm^2) via syringe pump (Harvard Apparatus) for up to 5 minutes, or were exposed to tracer media for equivalent timeframes under static conditions. Cells were continuously monitored and imaged after flow with a confocal microscope (Zeiss). Please see Supplementary Methods for additional details. The percentage of PMD-affected cells was quantified (Bioquant). Membrane uptake of FM dye during flow or residual intracellular dextran after flow were interpreted as evidence of PMD.

Mechanical wounding

MLO-Y4, OCY454, and primary osteocytes were wounded by glass beads, as previously described (8, 19), to facilitate wounding large numbers of cells. Vitamin E (Sigma T3251, 220 μM) (19) or calpeptin (Sigma C8999, 20 μM) (20) were introduced as indicated 24 hours prior to wounding. Whole cell lysates were collected for western blotting as previously described (21), using antibodies against c-fos (Santa Cruz) and β-actin (Sigma). Please see Supplementary Methods for additional details.

To assess cell survival after mechanical wounding, MLO-Y4 cells were wounded by glass beads in the presence of lysine-fixable fluorescein-conjugated dextran (10 kDa, 5 mg/mL +10 mg/mL BSA) containing either 1.8 mM Ca^{2+}, 1.8 mM Ca^{2+}+20 μM calpeptin, or 1.5 mM EGTA. Five minutes after wounding, cells were stained with propidium iodide (0.3 μg/mL) to detect dead cells (i.e., unrepaired PMD) and imaged on a multi-photon confocal microscope (Zeiss). Please see Supplementary Methods for additional details. The percentages of PMD-affected cells and dead cells were quantified (Bioquant).

Laser wounding – calcium signaling

MLO-Y4 cells were seeded 24 hours prior to experiments and loaded with Cal-520-AM as described (22). During incubation, treatments were introduced including: thapsigargin (Sigma T9033, 1 μM), gadolinium chloride hexahydrate (Sigma 203289, 10 μM), 18α

glycyrrhetinic acid (Sigma G8503, 75 μM), or apyrase (Sigma A6410, 10 U/mL), as indicated. A 3 μm laser PMD was created using a multi-photon laser, as described previously (19). Please see Supplementary Methods for additional details. Fluorescence was measured every second and normalized to baseline (pre-PMD) fluorescence (F/F_o) (6).

Laser wounding – repair dynamics

Cells were cultured for 24 hours in either normal culture medium, Vitamin C (1 mM) (19), Vitamin E (220 μM), or calpeptin (20 μM) (20). MLO-Y4 cells were subjected to laser wounding as described above and previously (9). Uptake of FM1-43 (2 μM±1.8 mM calcium) quantified osteocyte PMD repair rate as described (19).

Animal experiments – acute effects of downhill running

All experiments followed NIH guidelines and were approved by the Institutional Animal Care and Use Committee at Augusta University. Downhill treadmill running was selected as an *in vivo* mechanical stimulus, as it represents a physiological challenge that causes membrane disruptions in mechanosensitive tissues like myocytes (8, 9) and is a sufficient mechanical stimulus to induce bone adaptation in rodents (23). Female CD-1 mice (7 weeks old, Charles River) were permitted standard chow and water *ad libitum*. Mice were randomized by weight into treadmill running ("Loading") and control groups with only normal cage activity ("Control"). Mice acclimated to the treadmill (Columbus Instruments Exer3/6, 10 m/min, 10 min/day, −15° incline) for four days and received an injection of Evans Blue (50 mg/kg in PBS, intraperitoneal, Sigma) 18 hours prior to final experiments. Mice in the treadmill group were run downhill (−15°), where speeds were linearly increased from 10 m/min to 40 m/min over the course of 30 minutes. Control mice were exposed to the inactive treadmill. Mice were sacrificed by carbon dioxide within 2 hours after the treadmill run and were immediately perfused with 10% formalin. Longitudinal femoral frontal sections (7 μm) were prepared using CryofilmIIc (Section Lab) as previously described (21) and imaged with a multi-photon microscope (Zeiss), using FM1-43 to show cell membranes. Please see Supplementary Methods for additional details. For a subset of control and loaded animals, one humerus per mouse was processed and analyzed as described above. The percentage of cortical bone osteocytes with PMD (Evans Blue +FM1-43) was quantified (Bioquant). No signal for wavelengths used to detect Evans Blue occurred in un-injected animals (Supplemental Figure S1).

In a follow-up study to compare membrane wounding in a skeletal site presumed to be affected by treadmill loading (tibia) versus a site presumed to be unaffected by treadmill loading (calvaria), an additional group of female CD-1 mice (7 weeks old, Charles River) were trained, subjected to one bout of treadmill loading or control procedures, and sacrificed as described above. Tibias and calvaria (parietal bones) were decalcified in 15% EDTA for 14 days. Longitudinal frontal sections (tibia, 8 μm) and coronal sections (calvaria, 8 μm) were incubated overnight with a FITC-conjugated antibody against mouse albumin (AIFAG3140). Sections were mounted with DAPI (Vectashield H1500) and imaged with a confocal microscope (Zeiss). Please see Supplementary Methods for additional details. The percentage of cortical bone osteocytes with a PMD (albumin + DAPI) was quantified with (Bioquant).

Statistics

For each property, groups were compared by t-tests or 1-factor ANOVA followed by Student's t-test post-hoc analyses as appropriate using JMP 12.1.0 (SAS). Statistical significance was set at $p \leq 0.05$ for all comparisons. For quantification of histological/imaging studies, data were collected in a blinded fashion, and the same operator collected all data within a given experiment to limit inter-observer variability. Data are presented as mean ± standard error (SE), unless otherwise indicated. Sample sizes are indicated in each figure and/or caption.

Results

Osteocytes in vitro develop PMD in proportion to loading from fluid flow shear stress, and are preferentially produced by rapid loading

After exposure of osteocytes to shear stress using a Flexcell Streamer flow chamber, PMD events were detected by live-cell imaging as dextran-labeled osteocytes. Cells scored as positive for a PMD event exhibited dextran labeling of the cytosol that far exceeded the minimal (and punctate, peri-nuclear) fluorescence from endocytotic uptake in controls not exposed to flow but incubated for identical timeframes in the tracer medium (Figure 1A). Shear stresses between 10 to 30 dynes/cm^2 produced PMD in a dose-responsive fashion (Figure 1B). To determine the effect of loading rate on PMD development, MLO-Y4 cells were exposed to a 20 dynes/cm^2 shear stress either directly (1 step), or incrementally (2 to 13 steps) over a short timeframe (7 minutes total loading) (Figure 1C). PMD events were easily detected when the 20 dynes/cm^2 load was applied immediately, but significantly fewer were seen when load was applied gradually in step-wise fashion (Figure 1D).

Initial experiments were performed in the presence of 10% serum (5% FBS, 5% BCS), as reported previously (24), but because usage of low-serum medium is common in flow studies to negate potential confounding effects from serum (25), studies were repeated in the presence of 2% serum (1% FBS, 1% BCS). Similar (very low) levels of fluorescence were seen in static controls, and a comparable number of osteocytes were wounded by a 10 dynes/cm^2 fluid flow shear stress in 2% serum medium versus 10% serum medium (Figure 1E). A similar pattern of wounding, where rapid (direct) application of load caused more wounding than more gradual (incremental) application of loading, was seen in cells cultured in 2% serum medium versus 10% serum medium (Figure 1F).

We next imaged live cells during exposure to fluid shear using a flow chamber coupled to a microscope (Glycotech #31-001). Similar to results in the Streamer, dextran-labeled osteocytes were detected following as little as 5 minutes of a 30 dynes/cm^2 shear stress, but were not detected in static cultures (Figure 2A–B). Membrane uptake of FM dye, suggestive of PMD, was visible quickly upon initiation of flow (Figure 2C, arrows). Unlike fluorescent dextran, FM dye staining was limited to the membrane (as expected for lipophilic dye), and was most commonly seen on the osteocytic processes, consistent with osteocytes sensing load there (Figure 2C, arrows). Taken together, these data support the idea that osteocytes develop membrane tears with fluid flow and do so preferentially under rapid loading conditions.

Osteocytes in vivo develop PMD in response to treadmill exercise

We used treadmill running as a model of *in vivo* loading to determine if osteocytes experience PMD in response to mechanical stress *in vivo*. A baseline level of osteocytes labeled with Evans Blue, indicative of PMD, was detected in control mice, consistent with skeletal muscle where chronic but low-level membrane wounding occurs with normal locomotion (i.e., cage activity) (26) (Figure 3A). Importantly however, the number of PMD-labeled osteocytes was significantly (+277%) increased in the femur by downhill treadmill running, as also occurs in muscle (26) (Figure 3A). A similar pattern was observed in the humerus, which also experiences high peak loads during treadmill locomotion (Supplemental Figure S2) (27). These results were validated by immunohistochemical staining for endogenous albumin in tibias which demonstrated a nearly identical staining pattern (+209% labeled in loaded vs. control, Figure 3B). In skull calvaria, which should be minimally affected by treadmill locomotion (27), no difference in the number of PMD-labeled osteocytes was detected between loaded and control mice despite a clear increase in PMD-labeled osteocytes in the tibias of those same loaded mice (Figure 3C). Taken together, these data suggest that physiological loading in the form of treadmill running causes osteocyte membrane disruptions *in vivo* that can be observed via exogenous (Evans Blue) or endogenous (albumin) tracers.

PMD in vitro trigger mechanotransduction signaling that propagates to non-wounded neighboring osteocytes

After establishing that osteocytes develop membrane disruptions in response to loading both *in vitro* (Figure 1) and *in vivo* (Figure 3), we sought to determine if these disruptions initiate mechanotransduction. Calcium signaling is one of the earliest detectable responses in a mechanically wounded osteocyte (6), and we observed that osteocytes wounded by laser irradiation in Ca^{2+}-containing medium showed an immediate increase in intracellular Ca^{2+} similar in magnitude and timeframe to Ca^{2+} influx from fluid flow (28) (Figure 4A–B; Supplemental Movie 1 and 2). This Ca^{2+} wave spread rapidly to nearby, non-wounded cells, activating on average 45.2±4.1% of adjacent osteocytes (Figure 4A; Supplemental Movie 1). Thus, one wounded osteocyte initiated mechanotransduction in many non-wounded neighboring cells, providing a mechanism for amplification of a mechanosensation signal from a small wounded population. Initiation of calcium signaling in the wounded cell and survival of the wounded cell required extracellular Ca^{2+}, as EGTA treatment prevented Ca^{2+} signaling and led to rapid necrosis of the wounded cell (Supplemental Movie 3). However, death of the wounded cell from extracellular calcium chelation did not prevent Ca^{2+} signaling in adjacent cells, likely due to release of cytosolic molecules such as ATP from the wounded cell that have been previously reported to promote Ca^{2+} wave propagation (6). Indeed, development of a robust Ca^{2+} wave required both intracellular Ca^{2+} stores and ATP, as treatment with thapsigargin (Supplemental Movie 4) or apyrase (Supplemental Movie 5) inhibited propagation. Stretch-activated ion channels were not required as gadolinium chloride did not inhibit PMD-related Ca^{2+} signaling (Figure 4C; Supplemental Movie 6). Treatment with 18α-glycyrrhetinic acid (18α-GA) did not reduce signal transmission (Figure 4C; Supplemental Movie 7), suggesting gap junctions/hemichannels may not be involved. These data are consistent with previously reported bone cell Ca^{2+} responses to

loading (6), and demonstrate that PMD initiate Ca^{2+}-based mechanotransduction that spreads throughout an osteocyte population.

Downstream of Ca^{2+}, up-regulation of c-fos is a well characterized mechanotransduction response in bone cells. Mechanically-based injury (glass beads) wounded ~10% (150 mg beads, 10.7±2.3%) to ~50% (300 mg beads, 56.8±4.7%) of the cells (Figure 4D). This initiated an immediate (0 hr) and sustained (3 hr) increase in c-fos expression in MLO-Y4, OCY454, and primary osteocyte cells (Figure 4E). Taken together, these data show that PMD initiate mechanotransduction, and that PMD-affected cells and neighboring osteocytes may be primary participants in the response to mechanical stress.

Osteocyte PMD repair dynamics are similar to muscle cells

Repair of a membrane disruption is necessary for cell survival (29). We quantified influx of FM1-43 to measure osteocyte membrane repair rate, where faster repair is associated with a faster plateau in fluorescence over time (Figure 5A–B). Osteocytes rapidly repaired PMD in the presence of extracellular Ca^{2+} (“Control”) in approximately 60 seconds, which is comparable to normal repair rates in other cell types (Figure 5C). In contrast, repair was drastically inhibited in medium lacking physiological Ca^{2+}, and was mildly inhibited following treatment with calpeptin, a calpain inhibitor (Figure 5C). Osteocyte membrane repair rate was enhanced following culture the antioxidants Vitamin E or Vitamin C (Figure 5D). These data, which are consistent with myocyte behavior (19, 20), suggest osteocytes are capable of rapidly repairing membrane tears when they occur, and that repair rate can be modulated pharmacologically.

Altering osteocyte PMD repair affects mechanotransduction and survival

We bead-wounded osteocytes after culture in Vitamin E, which enhances PMD repair rate, and observed a blunted up-regulation of c-fos (Figure 5E). In contrast, culture in calpeptin (24 hrs, 20 μM), which slows PMD repair rate, enhanced up-regulation of c-fos stimulated by bead-induced PMD (Figure 5F). A completely unrepaired PMD should lead to cell death (29). To test this, we bead-wounded osteocytes after introducing repair-inhibiting agents EGTA and calpeptin (Figure 5C), and stained cells with propidium iodide 10 minutes after wounding to detect non-repaired (necrotic cells). Neither EGTA nor calpeptin treatment caused cell death in the absence of wounding in this timeframe (data not shown). With wounding, however, both calcium chelation by EGTA and inhibition of calpains by calpeptin significantly increased cell death after injury (Figure 5G). From these data, we propose that osteocyte PMD repair rate affects mechanotransduction, and that this rate can be modified to impact downstream signaling until a necrotic threshold is reached, as eventual repair of a PMD is necessary for cell survival (Figure 5H).

Discussion

Several osteocyte mechanosensation hypotheses have been developed based on *in vitro* experimentation, but their translation to *in vivo* models has been problematic (2–5). For example, fluid shear stress imposed *in vitro* opens osteocytic Connexin43 hemichannels promoting the release of prostaglandin E2 and ATP (18, 30), but cells from Connexin43-

deficient mice still respond to mechanical loading *in vivo* (31), and surprisingly, deletion of Connexin43 *in vivo* enhances (rather than abolishes) adaptation of bone to loading (32). Moreover, Connexin43 hemichannels are not opened in the osteocytic dendrites upon mechanical stimulation of the dendrites (33), whereas Ca^{2+} signaling is visible in the dendrites immediately upon dendritic stimulation (34). Similarly, while primary cilia are excellent candidate mechanosensors for osteocytes *in vitro*, the number of osteocytes presenting with primary cilia *in vivo* may be quite low (although conflicting evidence exists: (3, 35)). In this study, we asked whether *in vitro* mechanical loading from fluid shear stress or *in vivo* mechanical loading from treadmill running creates survivable plasma membrane disruptions (PMDs) in osteocytes, and if so, whether those membrane tears could initiate mechanotransduction in bone. These studies suggest that osteocytes do experience membrane disruptions, in proportion to the level of loading experienced (but most notably at high loads, discussed further below), and that these disruptions are capable of initiating mechanotransduction including Ca^{2+} signaling and expression of mechanoresponsive proteins like c-fos. Why might osteocytes employ such a mechanism? Evolution restricts musculoskeletal tissue growth to minimize the metabolic and biomechanical expense of excess tissue mass, which explains why mechanically regulated inhibitors of musculoskeletal growth (e.g., sclerostin and myostatin) exist. Likewise, we hypothesize that it could be evolutionarily beneficial for the initiating adaptation stimulus (mechanosensation mechanism) to specifically recognize injurious mechanical stressors (“no strain, no gain”), so tissue adaptation would be driven by a mechanobiological need to preserve cell viability and organ integrity.

It may seem surprising that osteocytes with membrane disruptions have not been detected in previous studies of osteocyte hemichannel function, where tracers (typically 10 kDa dextran) capable of highlighting a PMD by dye trapping are used as a negative control for Connexin-mediated dye transfer (30). However, we believe PMD-affected cells may have been missed in previous hemichannel experiments because they are usually performed in a non-physiologic, low Ca^{2+} or Ca^{2+}-free medium required for hemichannel opening; our studies demonstrate that Ca^{2+}-free conditions prevent PMD repair and cause post-wounding necrosis (Figure 5C, 5E), which would preclude detection of wounded cells by dye trapping. Importantly, with fluid flow under physiological conditions (i.e., medium containing Ca^{2+}), we observed dextran-labeled osteocytes that experienced PMD, underwent repair, and initiated mechanotransduction (Figures 1–4). It is possible that loading-induced PMD formation in osteocytes could be upstream of other well-known mechanotransduction mechanisms in bone. Calcium signaling is initiated at the exact site of deformation of the osteocytic cell membrane and rapidly propagates to the rest of the cell (34), a process identical to what we observed with membrane wounding which occurred even when stretch-activated ion channels were inhibited (Figure 4A, 4C). It is possible that loading-induced wounding of the osteocyte cell membrane allows for an initial influx of calcium, amplified through the release of intracellular calcium stores in the wounded and neighboring cells that could serve as the initiating stimulus for other downstream mechanotransduction events. This idea is consistent with the concept that extracellular calcium is required for loading-induced Ca^{2+} signaling in osteocytes (36), and would explain why wounded cells failed to induce Ca^{2+} signaling in EGTA-supplemented medium (Figure 4C, Supplemental Movie 3).

Intracellular Ca^{2+} stores and ATP were also important for signaling mechanisms downstream of osteocyte PMD (Figure 4C). These findings are consistent with previous studies demonstrating that a major mode for calcium wave propagation in a bone cell network is ATP released by the stimulated cell, which subsequently activates P2 purinergic receptors on the cell membrane and the PLC-IP3 pathway to promote release of endoplasmic reticulum calcium stores (6, 36).

It is important to note that while we observed osteocyte PMD formation occurred in proportion to the level of loading experienced *in vitro*, it was most readily detected at loading levels near or exceeding the range assumed to occur during normal physiological loading of bone (i.e., 0.8 to 3 Pa) (37). However, we note that recent modeling-based studies suggest that the shear stresses osteocytes experience *in vivo* may be much higher than this range due to lacunocanalicular geometry, with one study suggesting that maximum shear stresses may exceed 10 Pa (100 dynes/cm^2) within the canaliculi (38). Furthermore, we detected evidence of osteocyte membrane disruptions (intracellular albumin accumulation) following *in vivo* treadmill exercise, a loading model chosen because it represents a physiological challenge (8, 9) sufficient to induce bone adaptation to loading in rodents (23). Therefore, although osteocyte membrane disruptions occurred most appreciably at higher levels of loading, this mechanism may still hold great relevance for understanding the effects of *in vivo* loading on bone.

The 50 or more dendritic processes found on each osteocyte, which are physically tethered to bone matrix (39), would seem vulnerable to damage; as osteocytes predominantly sense mechanical loading via their processes (40), these two phenomena could be linked. If membrane tears do occur in the osteocytic processes and are responsible for some degree of mechanosensation, this could help explain why osteocytes are more sensitive to mechanical loading than osteoblasts, as this latter cell type lacks dendritic processes (24). We have not yet quantified whether membrane tearing occurs preferentially on the processes or cell body, although our *in vitro* observations suggest that wounding in the osteocyte processes is likely (Figure 2C). PMD create a disruption in the phospholipid bilayer, allowing entry of large molecules like albumin into the cytosol. However the physical mechanism of membrane tearing in osteocytes is not yet known. Two general possibilities include the direct effects of fluid flow-induced shear stress on the phospholipid bilayer, or the transmission of stress onto or through the bilayer via drag forces from pericellular or extracellular matrix proteins. Ongoing research will attempt to distinguish between these two possibilities. However, during our *in vitro* tests, we endeavored to ensure that no air bubbles were present in the flow system, as air bubbles can tear cells from the slide (thus potentially inducing a membrane disruption) (41). We cannot conclusively exclude the possibility of air bubbles in the Streamer tests because real-time visualization of the cells was not possible, but studies utilizing the Glycotech flow chamber, which showed a similar pattern of osteocyte membrane wounding, incorporated real-time imaging and were bubble free. Indeed, while we have observed that air bubbles can easily wound cells, those wounded cells rapidly delaminate from the slide and therefore should not have been present during post-flow imaging (data not shown).

In vitro studies revealed that osteocyte membrane disruptions developed in a dose-dependent fashion with fluid shear stress, particularly at higher levels of loading. Previous studies suggest that bone cells need an initial "stress kick" to properly respond to mechanical loading (42), and in line with this concept, PMD were most abundantly detected in osteocytes subjected to immediate physiological shear stress; ramping up to that level of loading decreased the number of PMD detected (Figure 1D, 1F). If PMD are upstream of signaling for skeletal adaptation, this behavior could help explain why more bone is formed via high-impact, rapid loading (e.g., gymnastics) as compared to low-impact, gradual loading (e.g., swimming) (43). *In vivo*, a low, chronic level of osteocyte membrane wounding occurred with normal cage activity as also occurs in muscle (9), which could represent one way bone detects routine loading (i.e., the absence of disuse). Importantly, however, osteocyte PMD were significantly increased by treadmill exercise, indicating that osteocytes experience PMD in response to increased mechanical loading *in vivo*. These data suggest that PMD may be upstream of mechanotransduction signaling for skeletal adaptation to loading. Areas of peak strain or strain gradients often best correlate with sites of bone adaptation (44), and therefore it would be of interest to know whether wounded osteocytes are located in areas of peak strain. We did not attempt to correlate PMD formation with peak bone strain in our treadmill loading studies, because while such analyses are straightforward with uniaxial loading models, more complex procedures like strain gauging or FEA modeling are required to ascertain areas of peak strain during gait (45), which was beyond the scope of the current study. In future work, we will quantify PMD formation from uniaxial loading (44) and determine whether PMD are correlated with areas of peak strain in these models. We chose treadmill exercise as a loading model despite its limitations because it represents a physiological challenge to the skeleton (natural loading motion from gait, no anesthesia required), promotes bone formation, and has been established to cause membrane disruptions in myocytes (9). We observed osteocyte wounding in both the hindlimbs and forelimbs. Most, but not all previous studies (27), have detected adaptation of the humerus to treadmill exercise including increased bone mineral content (46), bending strength (47), and cortical bone thickness (48).

In conclusion, these studies are the first to show the potential role of plasma membrane disruptions as a mechanosensation mechanism in osteocytes. As PMD repair failure in skeletal muscle leads to myopathy, explaining loss of muscle strength in a variety of conditions including diabetes (9, 49, 50), we anticipate that these results in bone may have direct physiological relevance for skeletal health; future studies will address whether failure of osteocyte PMD repair contributes to the development of osteodystrophy and osteoporosis (e.g., during aging), and will test therapeutic agents to modify PMD repair rates in bone to augment skeletal responses to loading.

Supplementary Material

Refer to Web version on PubMed Central for supplementary material.

Acknowledgments

Funding was received from the National Science Foundation (CMMI 1727949), the National Institute on Aging (P01 AG036675), the Medical College of Georgia at Augusta University, the Augusta University Medical Scholars

Program, and the Augusta University Student Training and Research (STAR) Program. The authors wish to thank Mr. Tim Kurtz and the Augusta University Cell Imaging Core Laboratory for assistance with imaging procedures and Drs. Mohammed Elsalanty and Regina Messer for assistance with the fluid flow studies.

References

1. Xiao Z, Quarles LD. Physiological mechanisms and therapeutic potential of bone mechanosensing. Rev Endocr Metab Disord. 2015; 16(2):115–29. [PubMed: 26038304]
2. Rosa N, Simoes R, Magalhaes FD, Marques AT. From mechanical stimulus to bone formation: A review. Medical engineering & physics. 2015; 37(8):719–28. [PubMed: 26117332]
3. Coughlin TR, Voisin M, Schaffler MB, Niebur GL, McNamara LM. Primary cilia exist in a small fraction of cells in trabecular bone and marrow. Calcified tissue international. 2015; 96(1):65–72. [PubMed: 25398598]
4. Malone AM, Anderson CT, Tummala P, Kwon RY, Johnston TR, Stearns T, et al. Primary cilia mediate mechanosensing in bone cells by a calcium-independent mechanism. Proceedings of the National Academy of Sciences of the United States of America. 2007; 104(33):13325–30. [PubMed: 17673554]
5. Xu H, Gu S, Riquelme MA, Burra S, Callaway D, Cheng H, et al. Connexin 43 channels are essential for normal bone structure and osteocyte viability. Journal of bone and mineral research : the official journal of the American Society for Bone and Mineral Research. 2015; 30(3):436–48.
6. Huo B, Lu XL, Costa KD, Xu Q, Guo XE. An ATP-dependent mechanism mediates intercellular calcium signaling in bone cell network under single cell nanoindentation. Cell Calcium. 2010; 47(3):234–41. [PubMed: 20060586]
7. Bakker AD, Silva VC, Krishnan R, Bacabac RG, Blaauboer ME, Lin YC, et al. Tumor necrosis factor alpha and interleukin-1beta modulate calcium and nitric oxide signaling in mechanically stimulated osteocytes. Arthritis Rheum. 2009; 60(11):3336–45. [PubMed: 19877030]
8. Grembowicz KP, Sprague D, McNeil PL. Temporary disruption of the plasma membrane is required for c-fos expression in response to mechanical stress. Molecular biology of the cell. 1999; 10(4): 1247–57. [PubMed: 10198070]
9. Labazi M, McNeil AK, Kurtz T, Lee TC, Pegg RB, Angeli JP, et al. The antioxidant requirement for plasma membrane repair in skeletal muscle. Free Radic Biol Med. 2015; 84:246–53. [PubMed: 25843658]
10. Hamrick MW, McNeil PL, Patterson SL. Role of muscle-derived growth factors in bone formation. Journal of musculoskeletal & neuronal interactions. 2010; 10(1):64–70. [PubMed: 20190381]
11. Lek A, Evesson FJ, Lemckert FA, Redpath GM, Lueders AK, Turnbull L, et al. Calpains, cleaved mini-dysferlinC72, and L-type channels underpin calcium-dependent muscle membrane repair. J Neurosci. 2013; 33(12):5085–94. [PubMed: 23516275]
12. Clark AG, Miller AL, Vaughan E, Yu HY, Penkert R, Bement WM. Integration of single and multicellular wound responses. Curr Biol. 2009; 19(16):1389–95. [PubMed: 19631537]
13. Bondesen BA, Mills ST, Kegley KM, Pavlath GK. The COX-2 pathway is essential during early stages of skeletal muscle regeneration. American journal of physiology Cell physiology. 2004; 287(2):C475–83. [PubMed: 15084473]
14. Wozniak AC, Anderson JE. Nitric oxide-dependence of satellite stem cell activation and quiescence on normal skeletal muscle fibers. Developmental dynamics : an official publication of the American Association of Anatomists. 2007; 236(1):240–50. [PubMed: 17117435]
15. Govey PM, Jacobs JM, Tilton SC, Loiselle AE, Zhang Y, Freeman WM, et al. Integrative transcriptomic and proteomic analysis of osteocytic cells exposed to fluid flow reveals novel mechano-sensitive signaling pathways. Journal of biomechanics. 2014; 47(8):1838–45. [PubMed: 24720889]
16. Ryan ZC, Craig TA, Salisbury JL, Carpio LR, McGee-Lawrence M, Westendorf JJ, et al. Enhanced prostacyclin formation and Wnt signaling in sclerostin deficient osteocytes and bone. Biochemical and biophysical research communications. 2014; 448(1):83–8. [PubMed: 24780398]
17. Spatz JM, Wein MN, Gooi JH, Qu Y, Garr JL, Liu S, et al. The Wnt Inhibitor Sclerostin Is Up-regulated by Mechanical Unloading in Osteocytes in Vitro. The Journal of biological chemistry. 2015; 290(27):16744–58. [PubMed: 25953900]

18. Genetos DC, Kephart CJ, Zhang Y, Yellowley CE, Donahue HJ. Oscillating fluid flow activation of gap junction hemichannels induces ATP release from MLO-Y4 osteocytes. Journal of cellular physiology. 2007; 212(1):207–14. [PubMed: 17301958]
19. Howard AC, McNeil AK, McNeil PL. Promotion of plasma membrane repair by vitamin E. Nat Commun. 2011; 2:597. [PubMed: 22186893]
20. Mellgren RL, Huang X. Fetuin A stabilizes m-calpain and facilitates plasma membrane repair. The Journal of biological chemistry. 2007; 282(49):35868–77. [PubMed: 17942392]
21. McGee-Lawrence ME, Carpio LR, Schulze RJ, Pierce JL, McNiven MA, Farr JN, et al. Hdac3 Deficiency Increases Marrow Adiposity and Induces Lipid Storage and Glucocorticoid Metabolism in Osteochondroprogenitor Cells. Journal of bone and mineral research : the official journal of the American Society for Bone and Mineral Research. 2016; 31(1):116–28.
22. Lock JT, Parker I, Smith IF. A comparison of fluorescent Ca(2)(+) indicators for imaging local Ca(2)(+) signals in cultured cells. Cell Calcium. 2015; 58(6):638–48. [PubMed: 26572560]
23. Hamann N, Kohler T, Muller R, Bruggemann GP, Niehoff A. The effect of level and downhill running on cortical and trabecular bone in growing rats. Calcified tissue international. 2012; 90(5): 429–37. [PubMed: 22466445]
24. Kamel MA, Picconi JL, Lara-Castillo N, Johnson ML. Activation of beta-catenin signaling in MLO-Y4 osteocytic cells versus 2T3 osteoblastic cells by fluid flow shear stress and PGE2: Implications for the study of mechanosensation in bone. Bone. 2010; 47(5):872–81. [PubMed: 20713195]
25. Klein-Nulend J, Burger EH, Semeins CM, Raisz LG, Pilbeam CC. Pulsating fluid flow stimulates prostaglandin release and inducible prostaglandin G/H synthase mRNA expression in primary mouse bone cells. Journal of bone and mineral research : the official journal of the American Society for Bone and Mineral Research. 1997; 12(1):45–51.
26. McNeil PL, Khakee R. Disruptions of muscle fiber plasma membranes. Role in exercise-induced damage. The American journal of pathology. 1992; 140(5):1097–109. [PubMed: 1374591]
27. Wallace IJ, Pagnotti GM, Rubin-Sigler J, Naeher M, Copes LE, Judex S, et al. Focal enhancement of the skeleton to exercise correlates with responsivity of bone marrow mesenchymal stem cells rather than peak external forces. J Exp Biol. 2015; 218(Pt 19):3002–9. [PubMed: 26232415]
28. Hung CT, Allen FD, Pollack SR, Brighton CT. Intracellular Ca2+ stores and extracellular Ca2+ are required in the real-time Ca2+ response of bone cells experiencing fluid flow. Journal of biomechanics. 1996; 29(11):1411–7. [PubMed: 8894921]
29. Cooper ST, McNeil PL. Membrane Repair: Mechanisms and Pathophysiology. Physiol Rev. 2015; 95(4):1205–40. [PubMed: 26336031]
30. Cherian PP, Siller-Jackson AJ, Gu S, Wang X, Bonewald LF, Sprague E, et al. Mechanical strain opens connexin 43 hemichannels in osteocytes: a novel mechanism for the release of prostaglandin. Molecular biology of the cell. 2005; 16(7):3100–6. [PubMed: 15843434]
31. Thi MM, Islam S, Suadicani SO, Spray DC. Connexin43 and pannexin1 channels in osteoblasts: who is the “hemichannel”? J Membr Biol. 2012; 245(7):401–9. [PubMed: 22797941]
32. Bivi N, Pacheco-Costa R, Brun LR, Murphy TR, Farlow NR, Robling AG, et al. Absence of Cx43 selectively from osteocytes enhances responsiveness to mechanical force in mice. J Orthop Res. 2013; 31(7):1075–81. [PubMed: 23483620]
33. Burra S, Nicolella DP, Francis WL, Freitas CJ, Mueschke NJ, Poole K, et al. Dendritic processes of osteocytes are mechanotransducers that induce the opening of hemichannels. Proceedings of the National Academy of Sciences of the United States of America. 2010; 107(31):13648–53. [PubMed: 20643964]
34. Adachi T, Aonuma Y, Tanaka M, Hojo M, Takano-Yamamoto T, Kamioka H. Calcium response in single osteocytes to locally applied mechanical stimulus: differences in cell process and cell body. Journal of biomechanics. 2009; 42(12):1989–95. [PubMed: 19625024]
35. Uzbekov RE, Maurel DB, Aveline PC, Pallu S, Benhamou CL, Rochefort GY. Centrosome fine ultrastructure of the osteocyte mechanosensitive primary cilium. Microsc Microanal. 2012; 18(6): 1430–41. [PubMed: 23171702]

36. Lu XL, Huo B, Chiang V, Guo XE. Osteocytic network is more responsive in calcium signaling than osteoblastic network under fluid flow. Journal of bone and mineral research : the official journal of the American Society for Bone and Mineral Research. 2012; 27(3):563–74.
37. Weinbaum S, Cowin SC, Zeng Y. A model for the excitation of osteocytes by mechanical loading-induced bone fluid shear stresses. Journal of biomechanics. 1994; 27(3):339–60. [PubMed: 8051194]
38. Verbruggen SW, Vaughan TJ, McNamara LM. Fluid flow in the osteocyte mechanical environment: a fluid-structure interaction approach. Biomechanics and modeling in mechanobiology. 2014; 13(1):85–97. [PubMed: 23567965]
39. Wang B, Lai X, Price C, Thompson WR, Li W, Quabili TR, et al. Perlecan-containing pericellular matrix regulates solute transport and mechanosensing within the osteocyte lacunar-canalicular system. Journal of bone and mineral research : the official journal of the American Society for Bone and Mineral Research. 2014; 29(4):878–91.
40. Han Y, Cowin SC, Schaffler MB, Weinbaum S. Mechanotransduction and strain amplification in osteocyte cell processes. Proceedings of the National Academy of Sciences of the United States of America. 2004; 101(47):16689–94. [PubMed: 15539460]
41. Stevens, HY., Frangos, JA. Bone Cell Responses to Fluid Flow. In: Helfrich, MH., Ralston, SH., editors. Methods in Molecular Medicine: Bone Research Protocols 80. Totowa NJ: Humana Press; 2003. p. 381-98.
42. Bacabac RG, Smit TH, Mullender MG, Van Loon JJ, Klein-Nulend J. Initial stress-kick is required for fluid shear stress-induced rate dependent activation of bone cells. Ann Biomed Eng. 2005; 33(1):104–10. [PubMed: 15709711]
43. Lima F, De Falco V, Baima J, Carazzato JG, Pereira RM. Effect of impact load and active load on bone metabolism and body composition of adolescent athletes. Med Sci Sports Exerc. 2001; 33(8): 1318–23. [PubMed: 11474333]
44. Niziolek PJ, Warman ML, Robling AG. Mechanotransduction in bone tissue: The A214V and G171V mutations in Lrp5 enhance load-induced osteogenesis in a surface-selective manner. Bone. 2012; 51(3):459–65. [PubMed: 22750014]
45. Prasad J, Wiater BP, Nork SE, Bain SD, Gross TS. Characterizing gait induced normal strains in a murine tibia cortical bone defect model. Journal of biomechanics. 2010; 43(14):2765–70. [PubMed: 20674920]
46. Kiuchi A, Arai Y, Katsuta S. Detraining effects on bone mass in young male rats. International journal of sports medicine. 1998; 19(4):245–9. [PubMed: 9657363]
47. Raab DM, Smith EL, Crenshaw TD, Thomas DP. Bone mechanical properties after exercise training in young and old rats. J Appl Physiol (1985). 1990; 68(1):130–4. [PubMed: 2312452]
48. Rooney SI, Loro E, Sarver JJ, Peltz CD, Hast MW, Tseng WJ, et al. Exercise protocol induces muscle, tendon, and bone adaptations in the rat shoulder. Muscles Ligaments Tendons J. 2014; 4(4):413–9. [PubMed: 25767777]
49. Bansal D, Miyake K, Vogel SS, Groh S, Chen CC, Williamson R, et al. Defective membrane repair in dysferlin-deficient muscular dystrophy. Nature. 2003; 423(6936):168–72. [PubMed: 12736685]
50. Howard AC, McNeil AK, Xiong F, Xiong WC, McNeil PL. A novel cellular defect in diabetes: membrane repair failure. Diabetes. 2011; 60(11):3034–43. [PubMed: 21940783]

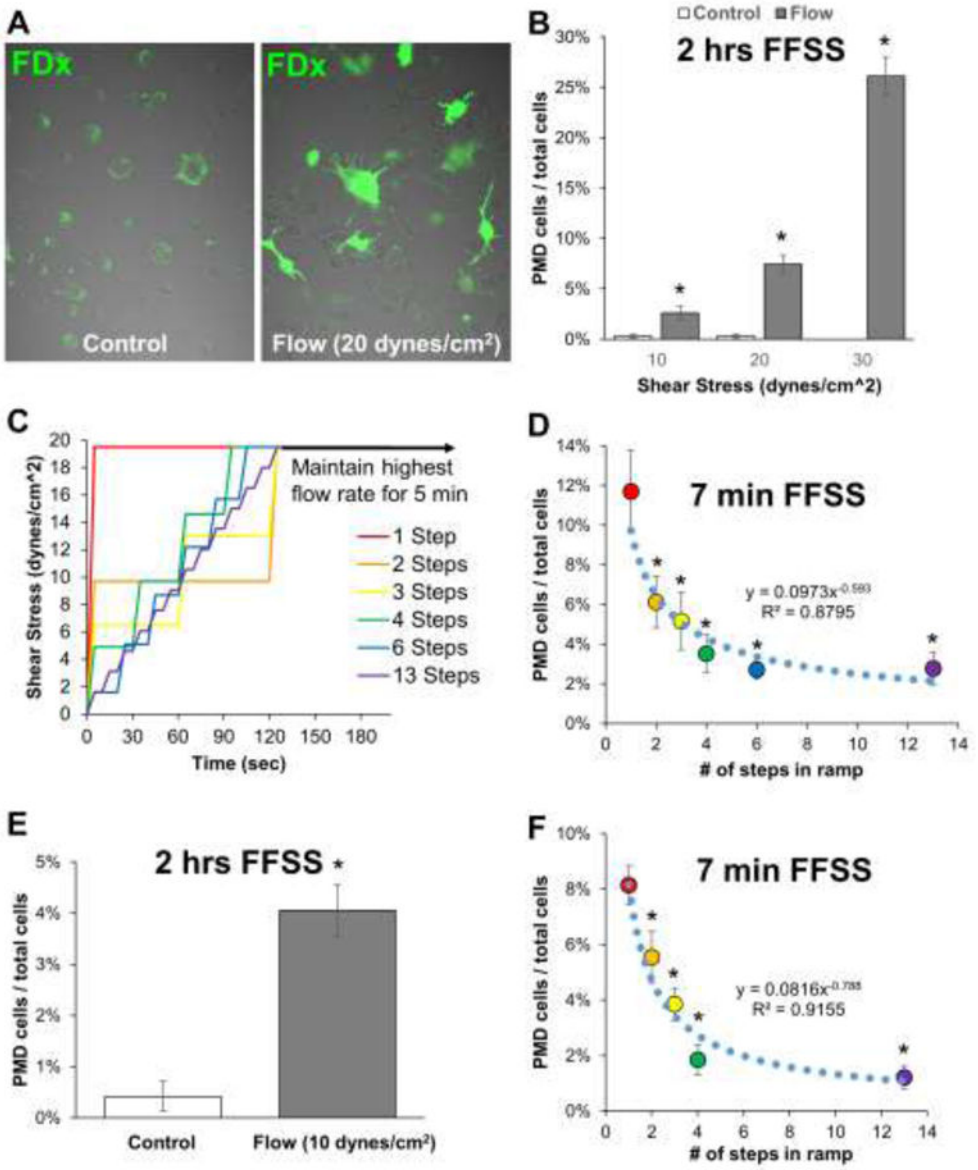

Figure 1. Osteocytes develop plasma membrane disruptions *in vitro* with fluid flow shear stress

A–B) MLO-Y4 osteocytes were loaded with various magnitudes of fluid flow shear stress for 2 hours using medium containing 5% FBS, 5% BCS, 1% penicillin/streptomycin, and 1 mg/mL fluorescein-conjugated dextran. PMD-labeled osteocytes (green) were quantified from randomly collected confocal microscopy images (n=10 to 12 images per condition) after rinsing samples thoroughly in PBS to remove residual dye. *p≤0.05 vs. control for each experiment; each control/flow pairing is representative of three independent experiments. C–D) A 20 dynes/cm^2 (2 Pa) shear stress was applied to MLO-Y4 osteocytes either immediately (1 step) or by gradually ramping up to this load (2 to 13 steps); PMD affected osteocytes were quantified as in panel B. *p≤0.05 vs. 1-step; representative of two independent experiments. E–F) Experiments in panels B and D were repeated with MLO-Y4 cells using medium containing 1% FBS, 1% FBS, 1% penicillin/streptomycin, 1 mg/mL

fluorescein-conjugated dextran, and 1 mg/mL bovine serum albumin. *p≤0.05 vs. control or 1-step, representative of four independent experiments.

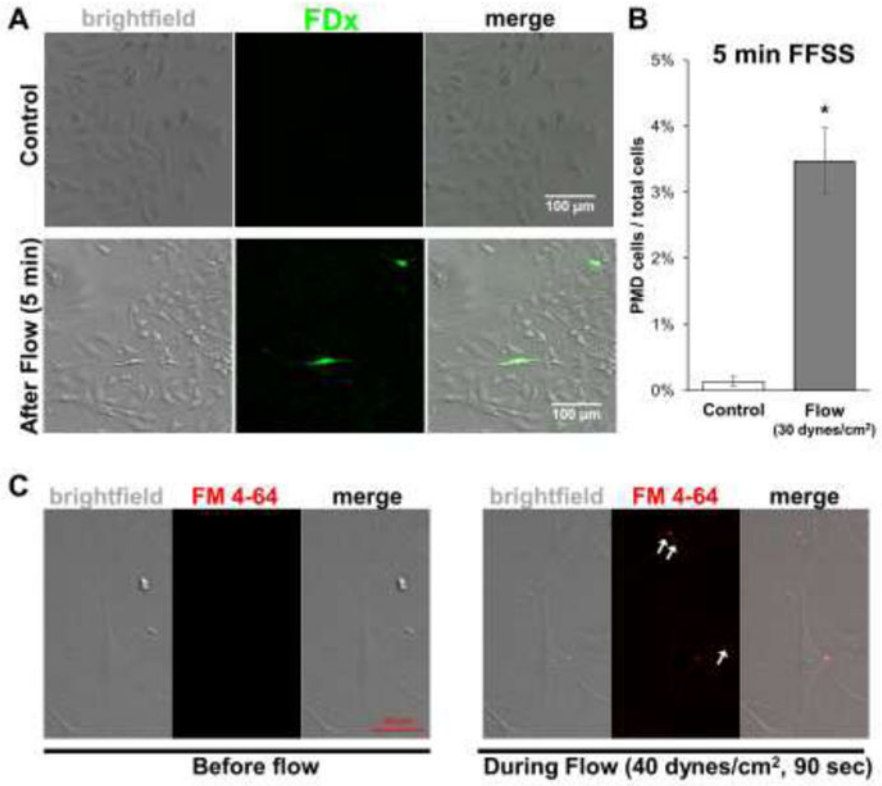

Figure 2. Formation of osteocyte plasma membrane disruptions can ve visualized during application of *in vitro* fluid flow shear stress

A) MLO-Y4 osteocytes were subjected to fluid flow shear stress (30 dynes/cm^2) for 5 minutes using culture medium (5% FBS, 5% BCS, 1% penicillin/streptomycin) containing 1 mg/mL fluorescein-conjugated dextran. Cells were imaged in real-time during flow, which confirmed the absence of air bubbles during testing. PMD-labeled osteocytes (green) were observed within the flow path after rinsing samples thoroughly in PBS to remove residual dye. B) PMD-labeled osteocytes (green) from experiments in panel A were quantified from randomly collected confocal microscopy images within the flow path (n=5 images per condition) after rinsing samples thoroughly in PBS to remove residual dye. *p≤0.05 vs. control; data represent mean ± SEM of five independent experiments. C)MLO-Y4 osteocytes were subjected to fluid flow shear stress (40 dynes/cm^2) using culture medium containing 2 µM FM4-64 dye, which permitted observation of membrane uptake of dye (white arrows) in real-time during flow loading. Each control/flow pairing is representative of three independent experiments.

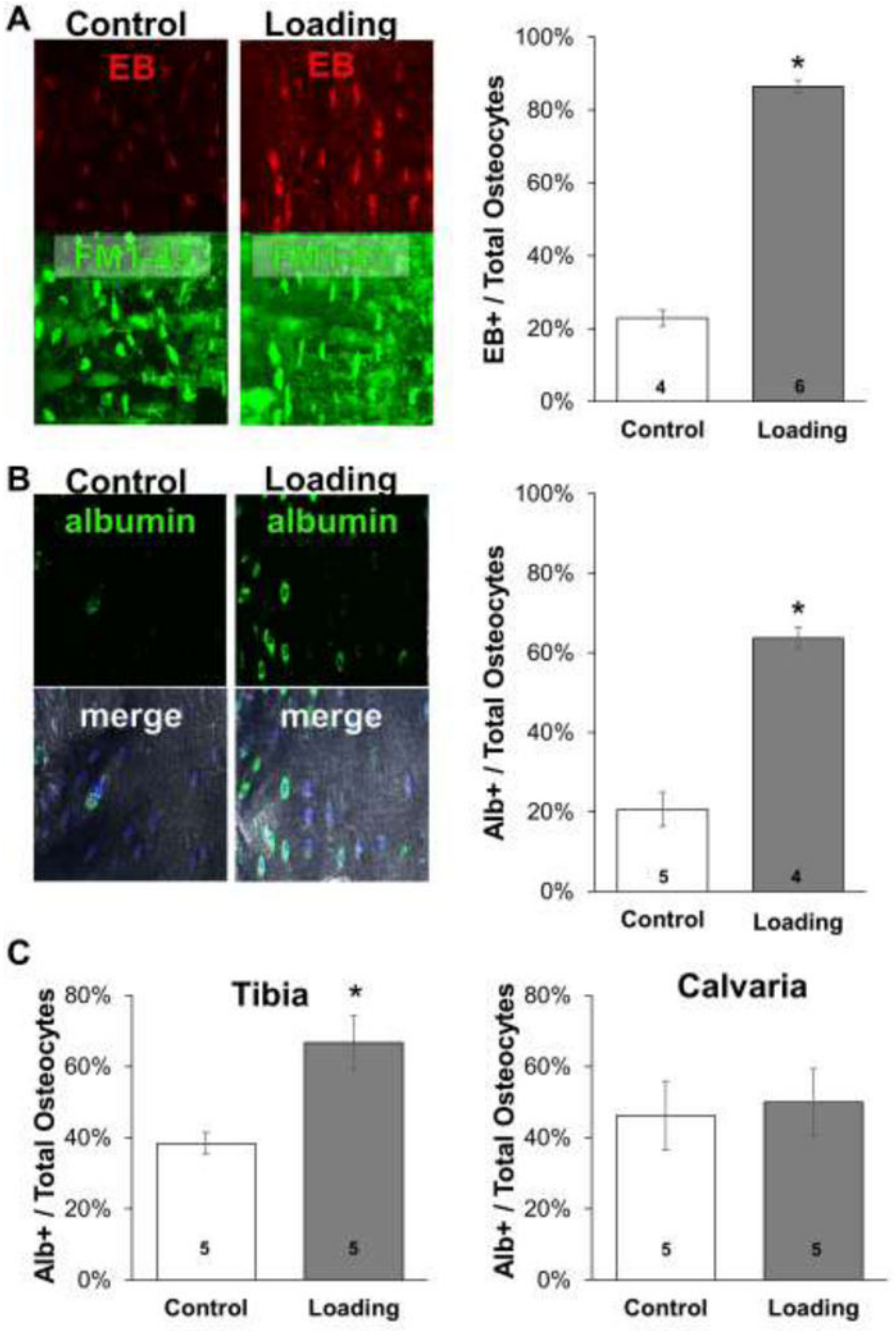

Figure 3. Osteocytes develop plasma membrane disruptions *in vivo* with treadmill loading

A) Female CD-1 mice were administered Evans Blue dye (50 mg/kg) as a membrane disruption tracer and either subjected to one bout of downhill treadmill loading ("Loading") or normal cage activity ("Control") as described in the Methods section. Longitudinal (frontal plane) femoral cryosections were prepared with Cryofilm IIc tape, using FM1-43 dye to label all cell membranes to ensure quantification of intracellular signals. Osteocytes presenting with a signal for Evans Blue and FM1-43 were quantified and normalized to the total number of FM1-43 stained osteocytes. EB: Evans blue dye. B) Tibias from the same animals described in panel A were decalcified, cryosectioned, and immunohistochemically

stained to detect endogenous albumin. Osteocytes presenting with a signal for FITC-labeled albumin and nuclear DAPI were quantified and normalized to the total number of DAPI-stained osteocytes; “merged” images represent FITC-conjugated antibody, DAPI, and differential interference contrast channels. C) Female CD-1 mice were subjected to downhill running or normal cage activity as in panel A. Tibias and calvaria were histologically prepared and quantified as in panel B. For each panel, *$p \leq 0.05$ vs. control; the number of mice in each group is indicated on each bar.

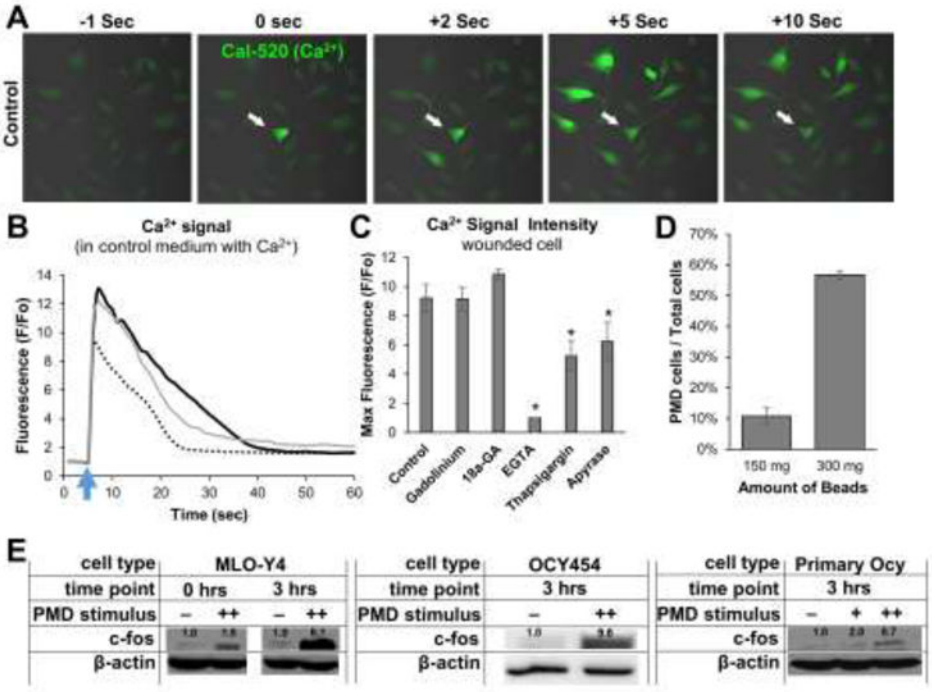

Figure 4. Plasma membrane disruptions initiate mechanotransduction in osteocytes

A–B) MLO-Y4 osteocytes were loaded with Cal-520-AM Ca^{2+} dye and a 3 μm diameter PMD was created via laser as described in the Methods. Cells were imaged every second beginning 5 seconds prior to wounding and concluding 60 seconds after wounding. A) White arrow shows PMD site; other cells were not wounded. B) Ca^{2+} curves from 3 representative cells cultured in control medium are shown to demonstrate Ca^{2+} signaling magnitude and duration following a PMD; blue arrow indicates time of PMD formation. C) Quantification of Ca^{2+} signal intensity in wounded cells treated with various inhibitors, *p≤0.05 vs. control. D) Quantification of the number of cells wounded by the glass bead mechanical wounding protocol described in the Methods for either 150 mg or 300 mg of beads added to each dish; cells were quantified as in Figure 1B. E) Expression of c-fos in PMD-affected MLO-Y4 cells, OCY454 cells, or immortalized primary osteocytes; numbers above each band show expression normalized to actin +: 150 mg beads, ++: 300 mg beads. Each panel representative of n≥3 experiments.

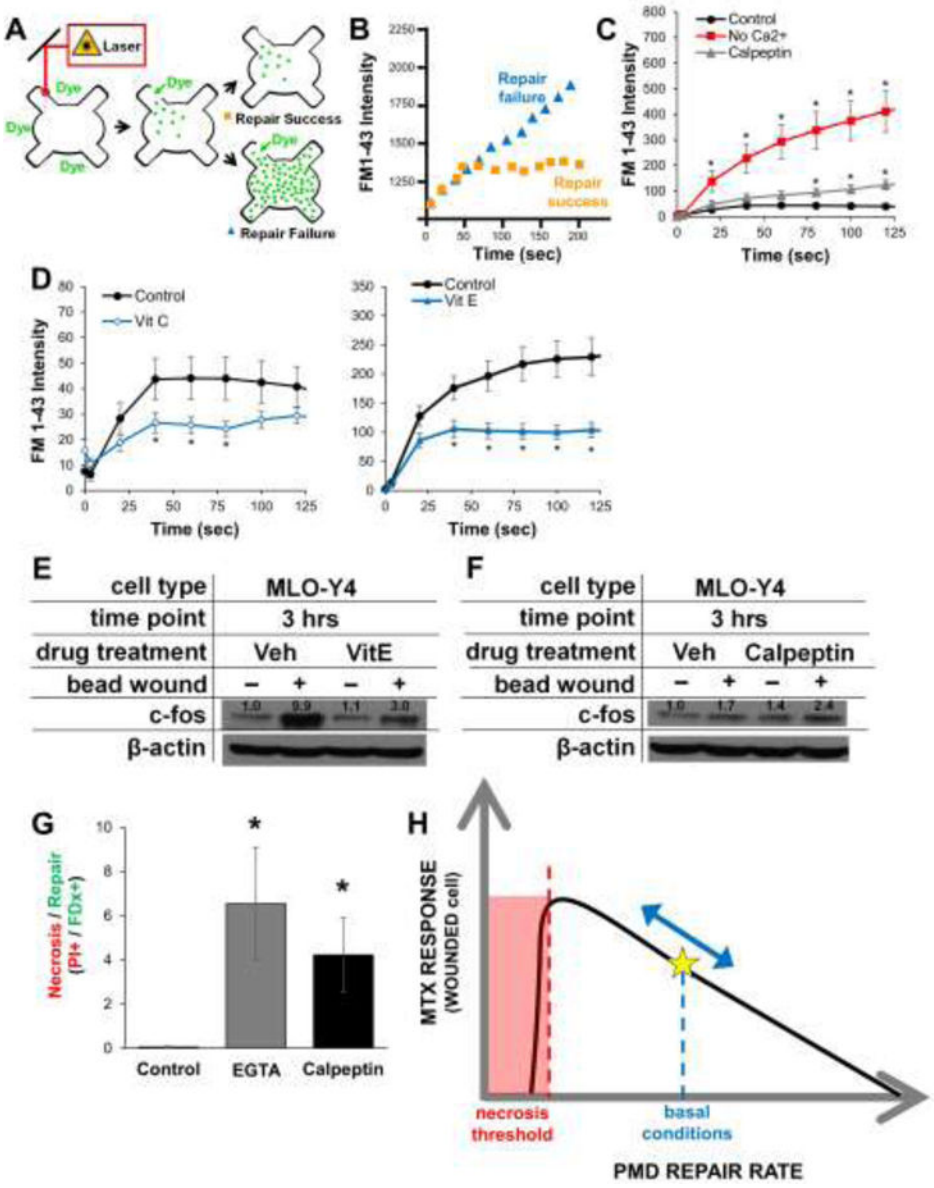

Figure 5. Osteocyte plasma membrane disruption repair rates can be enhanced or inhibited

A–B) Schematic describing the laser-based wounding assay for analysis of PMD repair rate. Influx of FM1-43 dye near the membrane disruption is used to quantify repair rate; a fast plateau in fluorescence indicates rapid, successful repair, whereas increasing fluorescence over time indicates slow repair or repair failure. C–D) MLO-Y4 cell PMD repair rates were impaired by removal of extracellular calcium or following culture in calpeptin (which inhibits the membrane-bound calpain molecules involved in PMD repair), but were enhanced following culture in the antioxidants Vitamin C or Vitamin E. *p≤0.05 vs. time zero, n>20 cells measured for each condition. E–F) MLO-Y4 cells were cultured in repair enhancing (Vitamin E) or inhibiting (calpeptin) for 24 hours prior to wounding; expression of c-fos was conducted as in Figure 4E. G) MLO-Y4 cells were cultured in repair-inhibiting agents as described in the Methods and subjected to mechanical wounding by glass beads as

described in Figure 4E. After wounding, cells were stained with propidium iodide to detect necrotic cells (i.e., unrepaired PMD) *p≤0.05 vs. control; 10 random images per condition were measured, and data are representative of three independent experiments. H) Proposed model for the influence of PMD repair rate on osteocyte mechanotransduction.